NANO MICRO small

Supporting Information

for *Small,* DOI: 10.1002/smll.202106172

A Dual-Cross-Linked Hydrogel Patch for Promoting Diabetic Wound Healing

Jing Liu, Moyuan Qu, Canran Wang, Yumeng Xue, Hui Huang, Qianming Chen, Wujin Sun, Xingwu Zhou, Guihua Xu,* and Xing Jiang**

Supporting Information

A Dual-Crosslinked Functional Hydrogel Patch for Promoting Diabetic Wound Healing

Jing Liu#, Moyuan Qu#, Canran Wang#, Yumeng Xue, Hui Huang, Qianming Chen, Wujin Sun, Xingwu Zhou, Guihua Xu*, Xing Jiang**

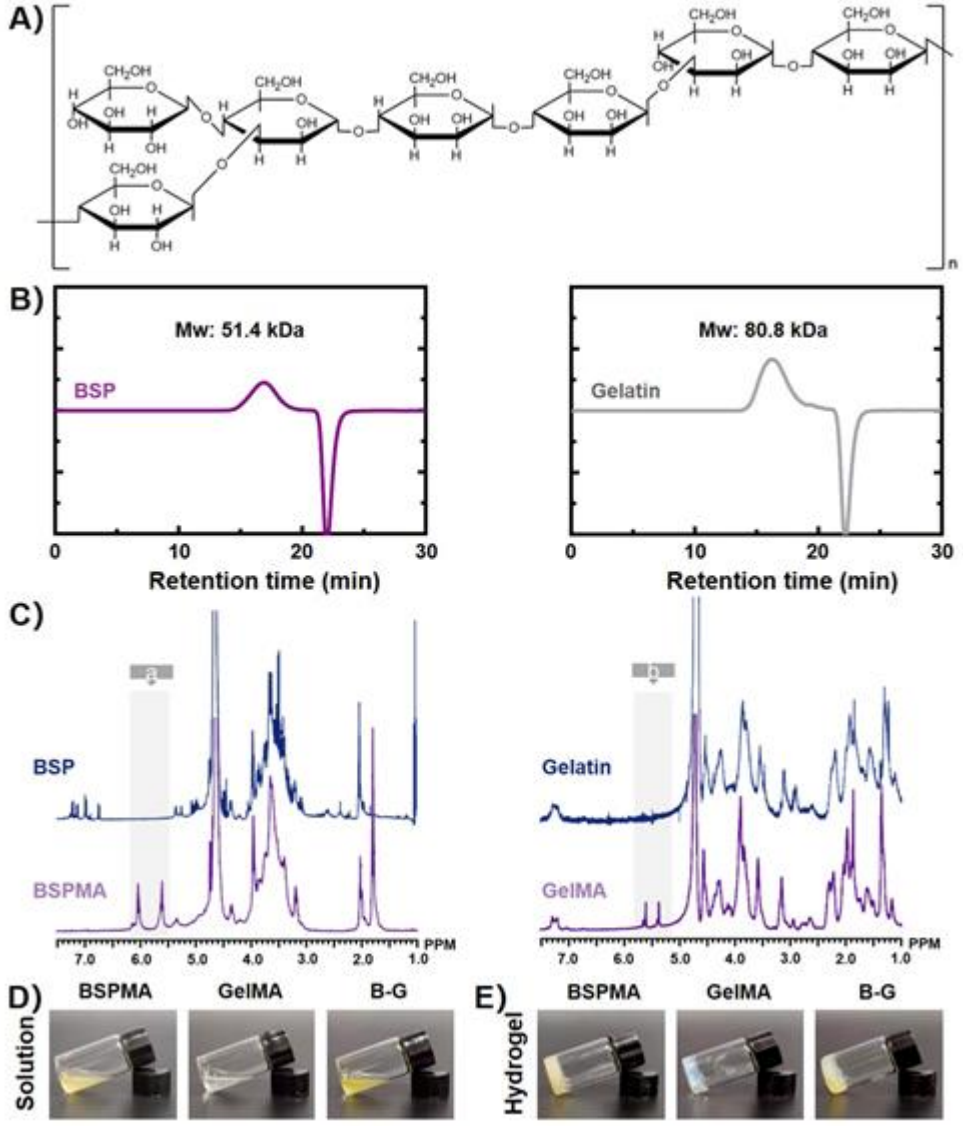

Figure S1. A) The chemical structures of *Bletilla Striata* Polysaccharide (BSP). B) Molecular weight of BSP and Gelatin measured by high-performance gel-filtration chromatography (HPGFC). C) ^{1}H-NMR spectra of BSP, BSPMA, Gelatin and GelMA. Peaks corresponds to acrylic protons of methacrylamide groups (a, and b). D) Photos of BSPMA, GelMA, and B-G solution and E) hydrogel after UV crosslinked for 15 s.

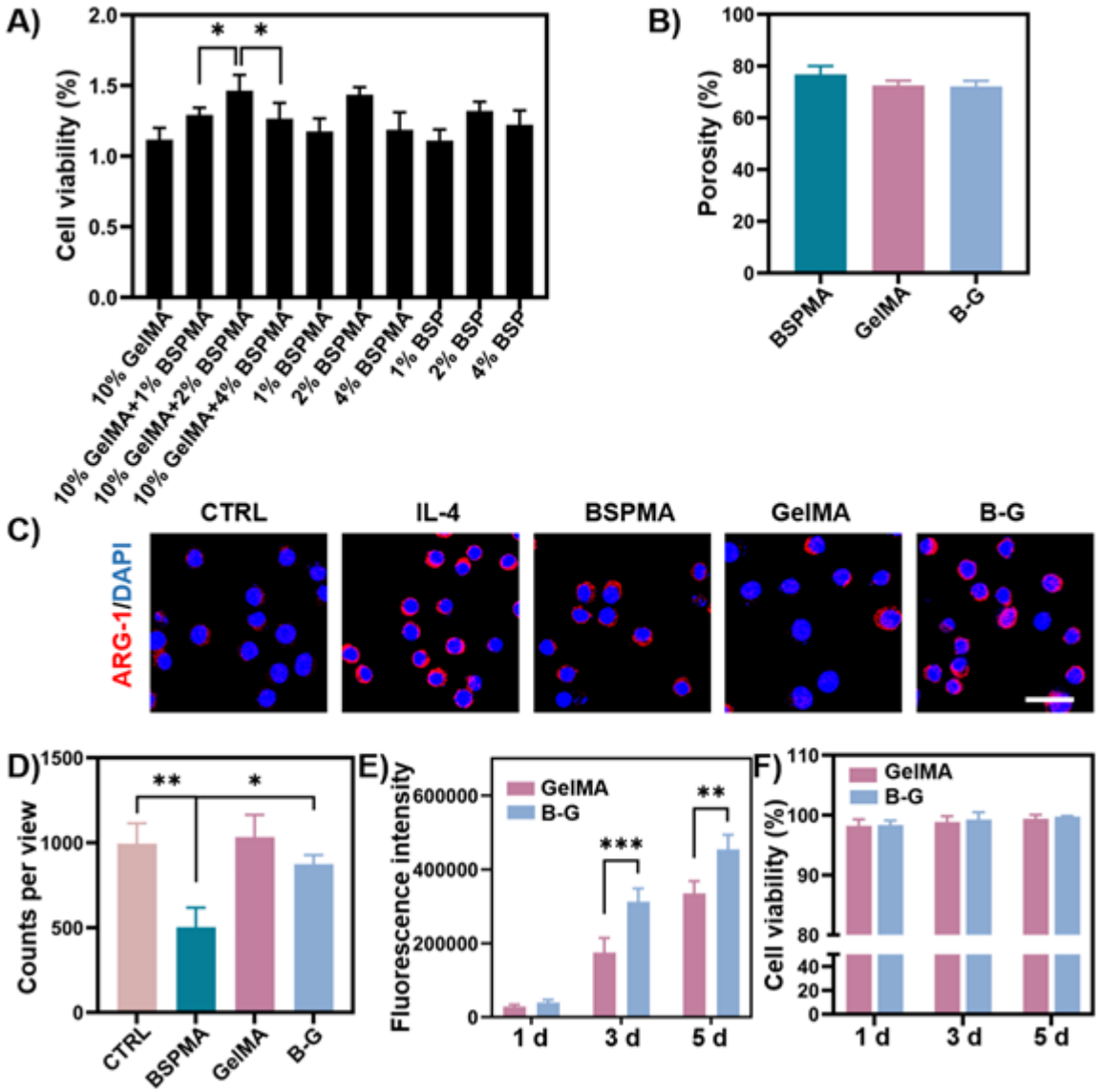

Figure S2. A) Cell viability when contacting with different mixtures (n = 3). B) Porosity of different hydrogels (n = 3). C) Immunofluorescent staining for ARG-1 (M2 marker) in RAW264.7 cells treated with LPS (control), IL-4 (positive control), BSPMA, GelMA and B-G hydrogel. (Scale bar = 50 μm). D) Statistical data of cells on TCP and hydrogels (n = 3). E) Quantification of fluorescence density of Live/Dead staining on day 1, 3, and 5 (n = 3). F) Cell viability of cells on GelMA and B-G hydrogel (n = 3). Data represent Mean ± SD; *p < 0.05, **p < 0.01, ***p < 0.001.

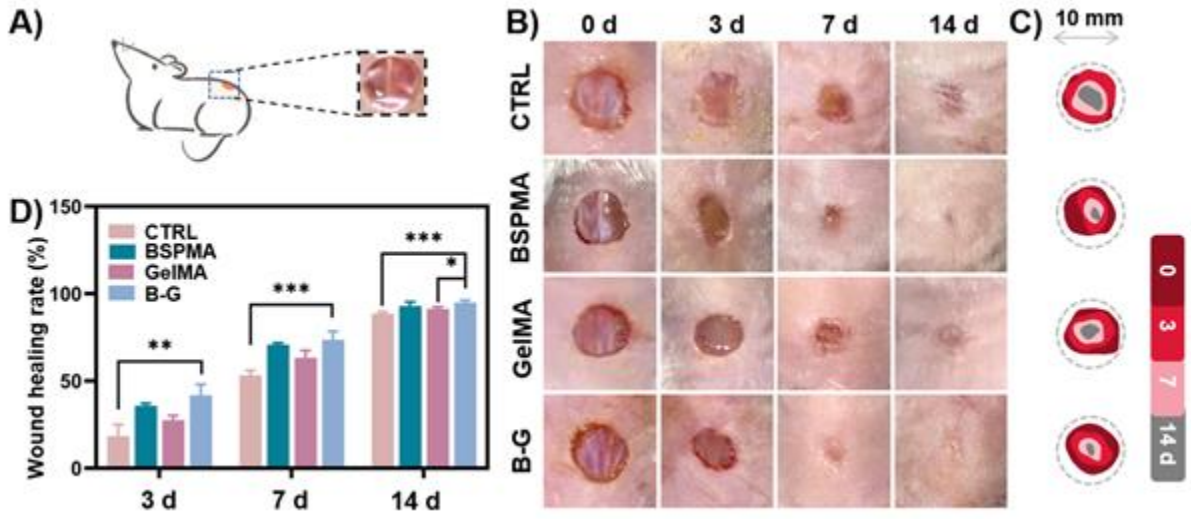

Figure S3. A) Schematic diagram of B-G hydrogel placed on the wound. B) Representative images of wound healing process in mice. C) Schematic diagram of the wound healed by different treatments for 14 days. D) Quantification of relative wound area at different time points (n = 3). Data represent Mean ± SD; *$p < 0.05$, **$p < 0.01$, ***$p < 0.001$.

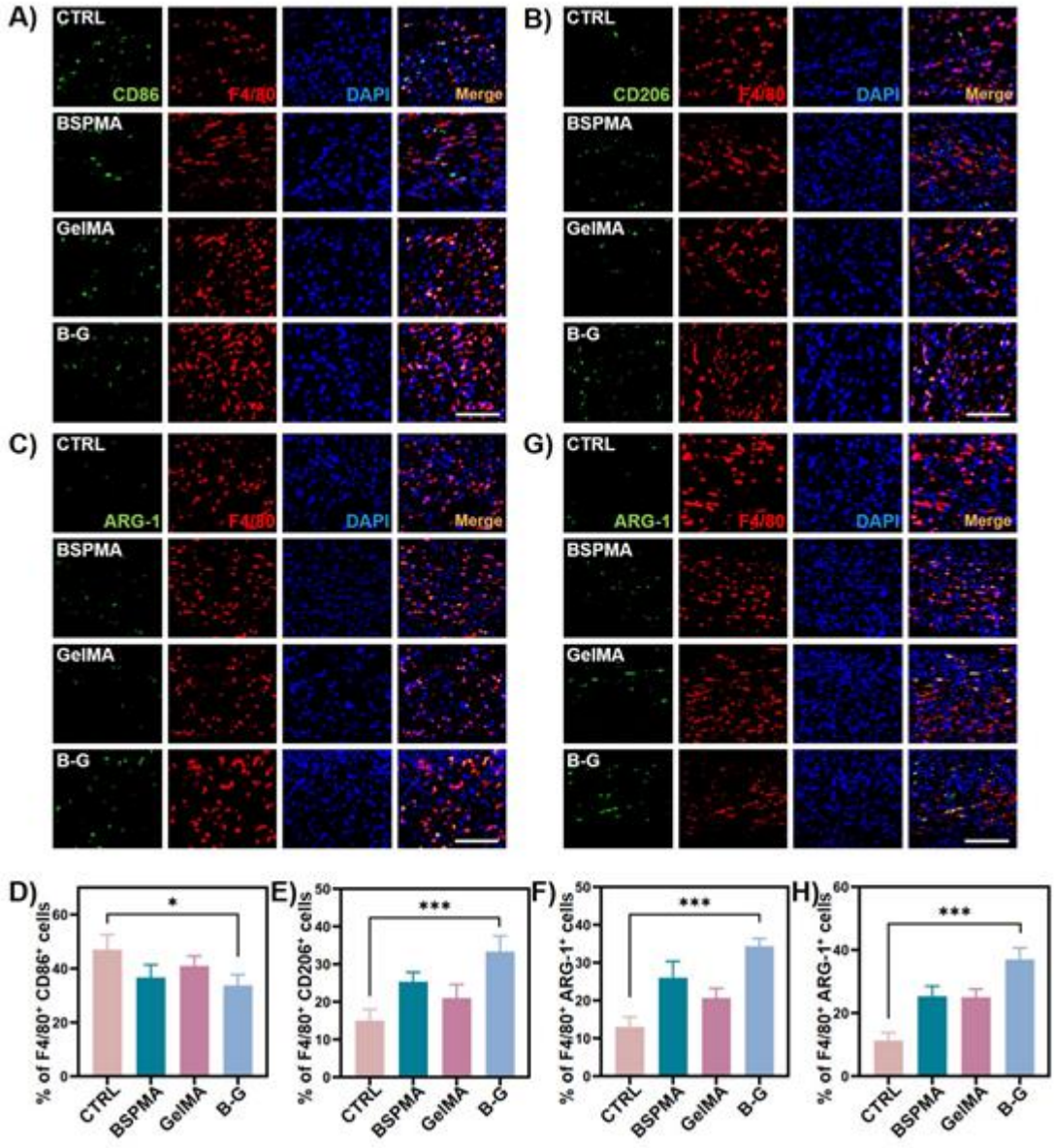

Figure S4. A-C) Immunofluorescent staining of wound bed tissues on day 3 post-treatment. M1 phenotype macrophage (CD86, green), M2 phenotype macrophage (CD206, green), M2 phenotype macrophage (ARG-1, green), F4/80 (red), and nuclei (DAPI, blue) (Scale bar = 100 μm). Statistical graph of the percentage of D) $F4/80^+$ $CD86^+$ M1 macrophages, E) $F4/80^+$ $CD206^+$ M2 macrophages, and F) $F4/80^+$ $ARG\text{-}1^+$ M2 macrophages on day 3 post-treatment. (n = 3). G) Immunofluorescent staining of wound bed tissues on day 7 post-treatment. M2 phenotype macrophage (ARG-1, green), F4/80 (red), and nuclei (DAPI, blue) (Scale bar =

100 μm). H) Statistical graph of the percentage of $F4/80^{+}$ $ARG\text{-}1^{+}$ M2 macrophages on day 7 post-treatment. (n = 3).

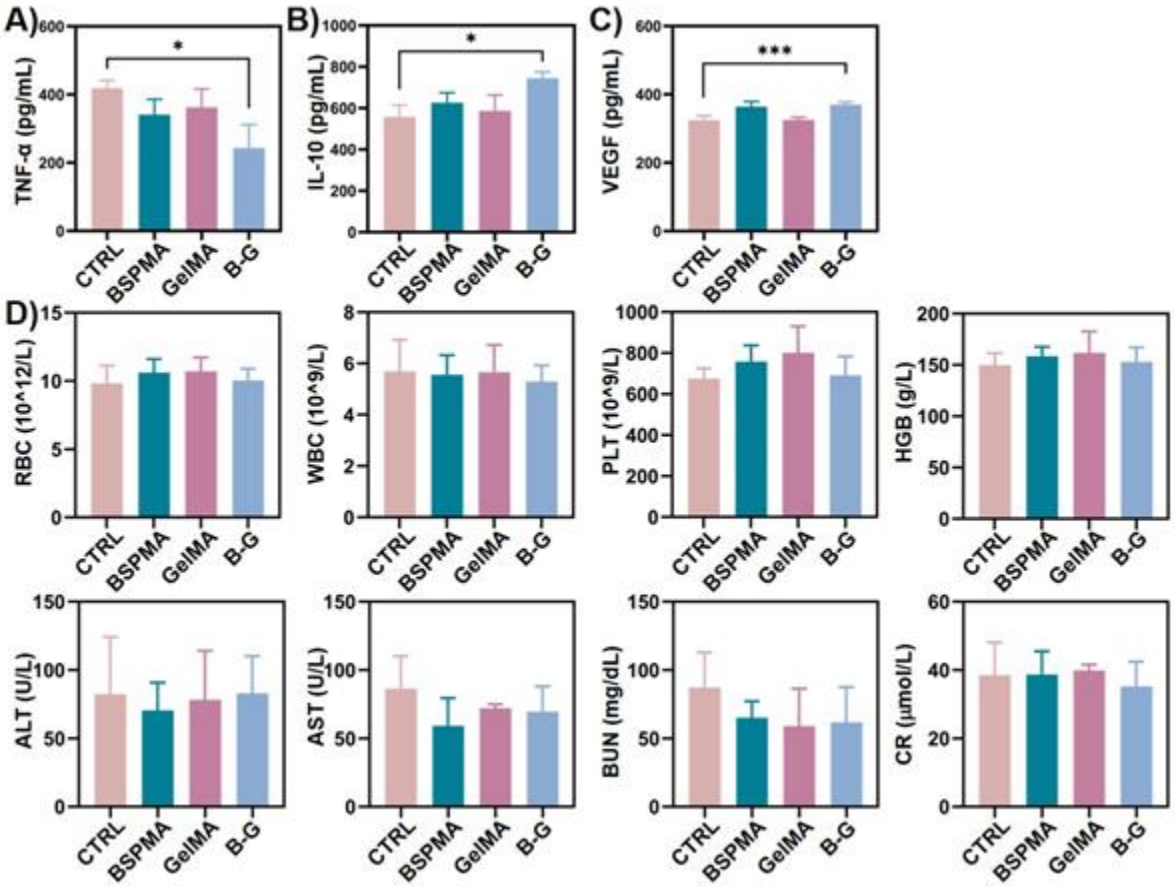

Figure S5. A) TNF-α concentrations in wound beds on day 7 (n = 3). B) IL-10 concentrations in wound beds on day 7 (n = 3). C) VEGF concentrations in wound beds on day 7 (n = 4). D) Biochemical and hematological factors of animals for control, BSPMA, GelMA, and B-G groups (n = 3). Data represent Mean ± SD; $^{**}p < 0.01$, $^{***}p < 0.001$.

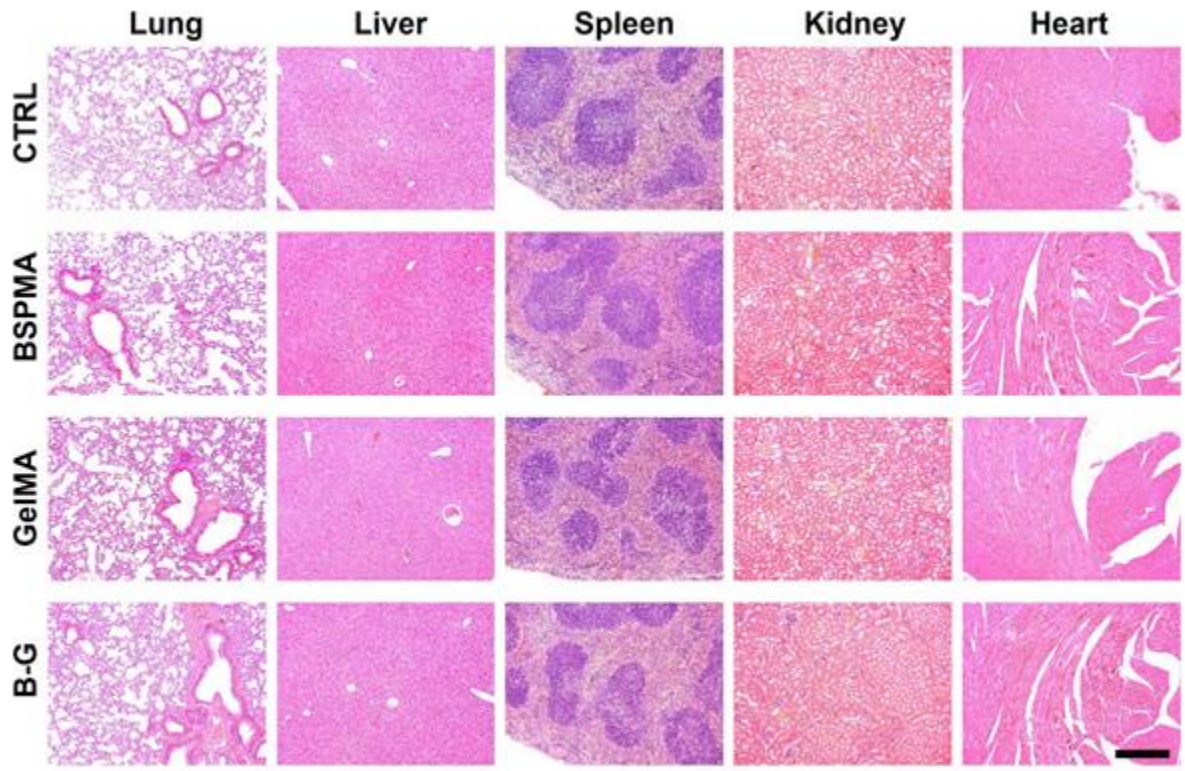

Figure S6. The H&E staining of Lung, liver, spleen, kidney, and heart in different groups (Scale bar = 250 μm).

Table S1 The primers used in Q-PCR analysis.

Genes	Forward primer	Reverse primer
GAPDH	AGGTCGGTGTGAACGGATTTG	TGTAGACCATGTAGTTGAGGTCA
TNF-α	CCCTCACACTCAGATCATCTTCT	GCTACGACGTGGGCTACAG
IL-10	GCTCTTACTGACTGGCATGAG	CGCAGCTCTAGGAGCATGTG
IL-6	CCACTTCACAAGTCGGAGGCTTA	CCAGTTTGGTAGCATCCATCATTTC
TGF-β	CAGTACAGCAAGGTCCTTGC	ACGTAGTAGACGATGGGCAG